Fiber array optical-coupling design issues for photonic beam formers

Kim, Jinkee, Riza, Nabeel

Jinkee Kim, Nabeel A. Riza, "Fiber array optical-coupling design issues for photonic beam formers," Proc. SPIE 2754, Advances in Optical Information Processing VII, (12 June 1996); doi: 10.1117/12.243136

SPIE.

Event: Aerospace/Defense Sensing and Controls, 1996, Orlando, FL, United States

Fiber array optical coupling design issues for photonic beamformers

Jinkee Kim and Nabeel A. Riza
Center for Research and Education in Optics and Lasers (CREOL)
and the Department of Electrical & Computer Engineering
University of Central Florida-Orlando
P. O. Box 162700, 4000 Central Florida Blvd., Orlando FL 32816-2700
Email: jkk@lorien.creol.ucf.edu

ABSTRACT

Novel two-dimensional (2-D) optical polarization switching array-based photonic time delay units (PTDUs) have been introduced for phased array antenna and wideband signal processing applications [1]. The use of low loss optical fibers allows remoting of the photonic beamformer, along with providing a compact, lightweight, and low electromagnetic interference (EMI) microwave frequency signal interconnection and distribution method, such as needed for very large aperture wide instantaneous bandwidth phased array antennas/radars. However, there are losses associated with multiple fiber interconnects that limit the maximum number of array channels in these systems. Thus, accurate analysis of such losses is crucial to the design of an optimal photonic fiber-based system. In this paper, we will present theoretical design and simulation results on optical fiber array interconnects for our 2-D N bit M channel photonic beamformer for wideband phased array antennas. In addition, we will discuss an alignment technique for the large channel count fiber arrays proposed for our beamformer that uses V-grooved silicon wafers. Note that these precise V-groove structures are fabricated via crystallographic perfection of the substrate, accurate alignment of the etch pattern with respect to the crystal planes, and optimized etch conditions. This paper will discuss these and other fiber array issues.

Keywords: fiber arrays, optical coupling, optical loss, phased array antennas

2. INTRODUCTION

In recent years, photonically controlled phased array antennas have been developed and studied in the area of radars and wireless communications. Key advantages of photonic beamformers are light weight, low loss, low crosstalk, potentially low cost, and high speed parallel processing. Photonic beamformer systems for phased arrays such as the bulk-optical controller proposed by Riza [1,2] require a large (>100) number of fiber interconnects that should be assembled with the lowest possible loss, and with the least assembly complexity and expense. By utilizing fiber interconnects, delay lines with very low crosstalk can be formed and further remoting of the phased array antenna is possible. The fiber array can be aligned to an microlens array. Thus, guided wave in the fiber is coupled in the air through microlens or graded-index (GRIN) rod lens collimators. The collimated parallel beams are processed through the PTDUs in our 2-D N bit M channel photonic beamformer for wideband phased array antennas [3]. The collimated beams can be re-coupled into fibers through the GRIN rod lenses to realize the long time delays or interconnects. However, there are losses associated with multiple fiber interconnects that limit the maximum number of array channels in these systems. Thus, accurate analysis of such losses is crucial to the design of an optimal photonic fiber-based system. One of the most important operations involved in a fiber optic system is the fiber core alignment to reduce power loss. Manufacturing tolerances on core eccentricity and fiber outer diameter can be tight to 1 to 2 μm or less. The fiber outer diameter is larger; i.e., 125 μm for a single mode (SM) fiber. Fiber tolerances during fabrication are well enough controlled to allow interconnects to use passive alignment of the fiber outer diameter by using the mature precision V-grooves substrates. The fiber array can be aligned with the collimator lens array.

The aim of this paper is to study fiber optic coupling issues and to design fiber arrays for photonic beamformers. This paper describes theoretical design and simulation results on fiber array interconnects for our 2-D N bit M channel photonic beamformer. In section 3, single-mode fiber coupling efficiency with GRIN rod lenses is studied in terms of lateral, angular, and separation misalignment of the fiber-optic GRIN lens assembly. In section 4, fiber-optic GRIN-based coupling efficiency issues when using external imaging lenses are studied to reduce the coupling loss for long separation

between two array assemblies. Experimental results to simulate the 2-D N bit M channel photonic beamformer will be discussed. The detailed theoretical calculation will appear in a future publication. In section 5, the design of fiber-optic graded-index (GRIN) rod lens or microlens arrays will be described.

3. SINGLE-MODE FIBER COUPLING EFFICIENCY WITH GRADED-INDEX ROD LENSES

A GRIN lens is used to transform the light from an optical fiber into a collimated beam, and a second GRIN lens is used to focus the collimated beam onto a second fiber in an expanded beam connector. Such an arrangement is shown in Fig. 1 using two quarter-pitch GRIN rod lenses where w_i's are beam radius ($1/e^2$ of its peak intensity) at various spots along the propagation direction. The quarter-pitch GRIN lenses serve as collimating and focusing devices which are sold under the trade name SELFOC by Nippon Sheet Glass Co., Ltd. [4]. The excellent collimating and focusing properties of these lenses make them useful for coupling laser diodes and light-emitting-diodes (LEDs) to fibers, and fibers to avalanche photodiodes (APDs) and detectors. There are many potential advantages of this expanded beam configuration. The primary advantage of the GRIN fiber-to-fiber system is the large allowable separation without additional optics between the interconnecting fibers. For example, in a fiber-to-fiber connector, a separation between fibers of a fiber diameter results in a loss of approximately 1 dB [5]. With fiber collimators, the fibers can be separated by several thousand core diameters with minimum loss. Also, the effects of dirt and contamination are reduced due to the relatively large size of the beam compared to direct connections of two ends of fibers (butt-joint connections). Fiber-to-lens alignment must be done to the same accuracy as fiber-to-fiber alignment in butt-joint connectors. Another advantage of some expanded beam configurations is that anti-reflection (AR) coating can be easily applied to the lens surfaces, reducing Fresnel loss from 9% to less than 0.5% [4]. The high quality AR coatings cannot be applied to a single fiber or fibers terminated in glass tubes due to the small area of the fiber end-face.

Reduced sensitivity to longitudinal lens-to-lens separation is dependent on the degree of collimation determined by the degree of aberration and the quality of the lenses. Fiber-to-lens sensitivity to lateral offset is approximately the same as for butt-joint connectors. Sensitivity of lens-to-lens angular misalignment is increased compared to butt-joint connections, which again is approximately equal to the fiber-to-lens sensitivity [6,7].

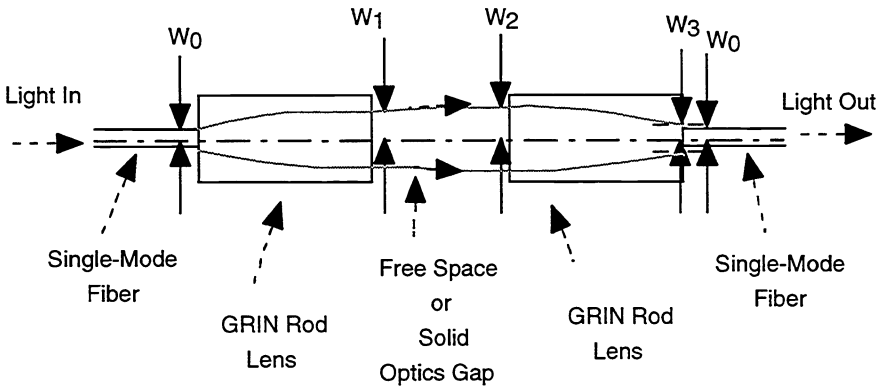

Fig. 1. Output beam from the first GRIN lens expands in the air gap, producing an enlarged image on the receiving fiber.

The next sub-section describes calculations of SM fiber coupling efficiency with GRIN rod lens. Recently, Gilsdorf and Palais [6] reported reasonably accurate formulas for this problem. In this paper, the same formulas are used to calculate and match experimental results at a wavelength 0.6328 μm.

3.1 Theoretical Coupling Loss

It is important to analyze the power loss of fiber collimators due to misalignment between transmitting and receiving GRIN lenses. As shown in Fig.2, there are three types of misalignment: (1) offset X_0 between the longitudinal axes of the lenses, (2) separation Z between the faces of the lenses, and (3) angular tilt θ between the longitudinal axes of the lenses.

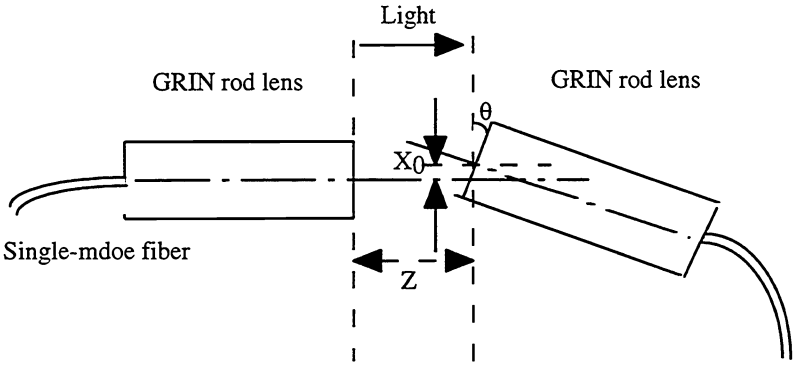

Fig. 2. Alignment factors for GRIN rod lenses are lateral offset X_0, separation Z, and angular tilt θ.

A lateral offset between the two GRIN rod lenses causes loss because the rays incident upon the output fiber are tilted and some of these rays lie outside the acceptance angle of the receiving fiber. Additional losses result from the expansion of the Gaussian beam as it propagates through the air gap from the transmitting GRIN lens to the receiving GRIN lens. The spot size of the beam expands in the gap according to the relation [8]

$$w_2(Z) = w_1[1+(\frac{\lambda Z}{\pi n w_1^2})^2]^{1/2}, \tag{1}$$

$$w_1 = \frac{NA}{n_0\sqrt{A}}, \tag{2}$$

where λ is the wavelength of light, n is the index of refraction in the gap, Z is the gap length, w_1 is the radius of the output beam, NA is the numerical aperture of the SM fiber, n_0 is the refractive index on the axis of the lens, and $\sqrt{A}$ is the gradient constant defined on a per mm basis (i.e., mm^{-1}).

The excess optical loss in decibels due to misalignment is

$$L = -10\log\left[\frac{E(X_0,Z,\theta)}{E(0,0,0)}\right]^2, \tag{3}$$

where E(0,0,0) is the coupled field with perfect alignment. The overlap $E(X_0,Z,\theta)$ between the image from the input fiber and the SM Gaussian-field profile of the output fiber at the face of the output fiber is calculated by the use of a double integral. The formulas for the coupled field that are due to misalignments are [6]

$$E(X_0,0,0) = \int_{-\infty}^{+\infty}\int_{-\infty}^{+\infty}\exp\left[-\frac{(x+X_0)^2+y^2}{w_1^2}\right]\cdot\exp\left[-\frac{x^2+y^2}{w_1^2}\right]dx\,dy \tag{4}$$

for lateral offsets,

$$E(0,Z,0) = \int_{-\infty}^{+\infty}\int_{-\infty}^{+\infty}\exp\left[-\frac{x^2+y^2}{[w_3(Z)]^2}\right]\cdot\exp\left[-\frac{x^2+y^2}{w_0^2}\right]\left[\frac{1}{w_3(Z)}\right]^2 dx\,dy, \tag{5}$$

$$w_3 = \frac{w_2 w_0}{w_1}, \tag{6}$$

for separation, and

$$E(0,0,\theta) = \int_{-\infty}^{+\infty}\int_{-\infty}^{+\infty} \exp\left[-\frac{(x+D_\theta)^2 + y^2}{w_0^2}\right] \cdot \exp\left[-\frac{x^2+y^2}{w_0^2}\right] dx\, dy, \tag{7}$$

$$D_\theta = \frac{\tan\theta}{n_0\sqrt{A}}, \tag{8}$$

for angular tilt.

3.2 Theoretical and Experimental Results

Figs. 3,5, and 6 show theoretical and measured experimental optical losses for the misalignment issues related to separation, lateral offsets, and angular tilt, respectively. In this paper, two wavelengths of 0.6328 μm and 1.3 μm are considered. For the wavelength of 1.3 μm, the theoretical and experimental results were reported in Ref. 6. For the wavelength of 0.6328, the theoretical and experimental results are investigated in this paper to help the understanding of the behavior of the fiber-GRIN rod lens assemblies. For the two wavelengths 0.6328 μm and 1.3 μm, refractive indices on axes of 1.6071 and 1.5916, gradient constants of 0.3388 mm^{-1} and 0.327 mm^{-1}, and mode-field diameter of 4.6 μm and 10.5 μm are used, respectively [4]. In all figures, solid lines and dotted lines denote results for 0.6328 μm and 1.3 μm, respectively. For the wavelength of 1.3 μm, the same theoretical results were obtained as in the Ref. 6. In our experiments, 0.6328 μm wavelength was used. A set of two single-mode fiber pigtailed GRIN rod lenses (N.A. : 0.11, radius R_0 = 0.9 mm, λ = 0.6328 μm) were used as the source and receiving channels. The light is detected at the end of the receiving fiber. A distance of less than 3 mm was maintained between the detector and the end of the receiving fiber pigtailed during measurement. The accuracy of the optical power detector manufactured by Newport Corp. was 2%. The optical loss (dB) is calculated as 10 log (I_R /I_S) [dB] where I_R is optical power in mW measured at the output of the coupled or receiving fiber-GRIN assembly, and I_S is optical power in mW measured at the output of the receiving fiber-GRIN assembly when other factors such as the lateral offset and the angular tilt are perfectly aligned. Theoretical calculation shows a good agreement with the measured data for the short separation (< 400 mm), as shown in Fig. 3, where calculated power losses due to the separation Z of 1000 mm are 22 dB and 33 dB for the wavelengths of 0.6328 μm and 1.3 μm, respectively. These losses result from beam-width broadening due to diffraction. At the separation Z of 200 mm, the calculated optical loss is 3.5 dB. This value is used to calibrate the other losses due to the lateral offset and the angular tilt, since the separation between the two source and receiving GRIN lens was 200 mm for the other experiments.

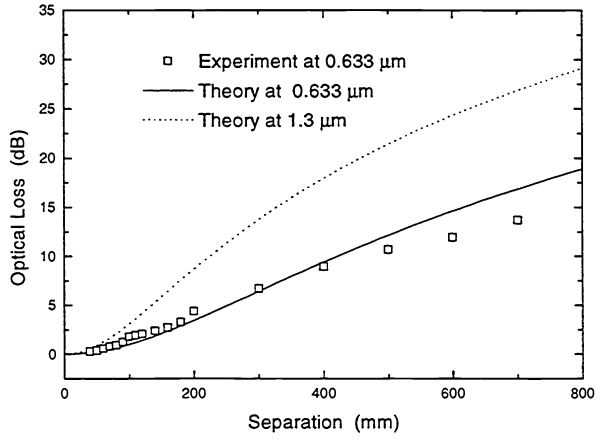

Fig. 3. Optical loss as a function of separation between the two GRIN lenses.

Fig. 4 shows calculated diffracted beam radii as a function of propagation distance for the wavelengths of 0.6328 μm and 1.3 μm. As seen in Fig. 4, a broader beam width is obtained for the longer wavelength diffraction. At the propagation distance of 1000 mm, the beam radius for the wavelength of 1.3 μm is 2 mm, resulting in a large loss (i.e., 33dB). Beam radii at 50 mm for both wavelengths are expanded less than 10% of the initial beam radii. The small diffraction of the Gaussian beam out of the GRIN rod lens allows placement of many optical components such as polarizers, spatial light modulators (SLMs), and beamsplitters, between the source and receiving GRIN assemblies. The loss due to the separation of GRIN lenses can be reduced by employing imaging lenses between two GRIN rod lenses, as originally proposed in [9]. Fig. 5 shows calculated and measured optical loss as a function of the lateral offset between the two GRIN lenses. Measured optical loss is represented by squares as a function of lateral offset between the two fiber-GRIN assemblies when the separation between the two GRIN lenses is 20 cm. Due to this separation of 200 mm in this experiment, the measured data was compensated with a theoretical separation optical loss of 3.5 dB. As shown in Fig. 5, about 3 dB losses were calculated with 0.18 mm lateral misalignment for both wavelengths. Thus, in an optical beamformer system, when using the GRIN-based coupling approach, the lateral misalignment must be minimized appropriately via lateral alignment correction optics and/or mechanical fixtures. The measured excess optical loss at the lateral offset of 0.3 mm matches the theoretical loss of 9 dB. Both the theory and the experimental results show reasonable agreement.

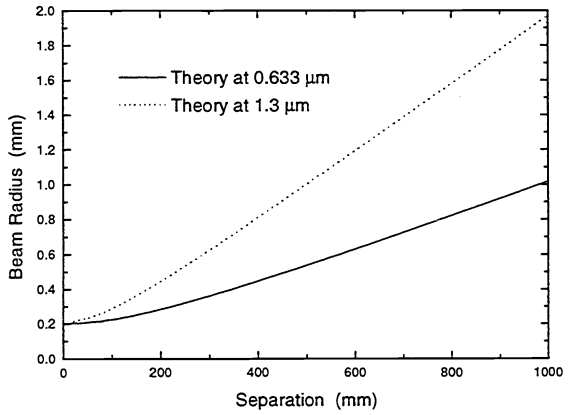

Fig. 4. Calculated beam radius at the input of the receiving GRIN lens as a function of separation between the two GRIN lenses

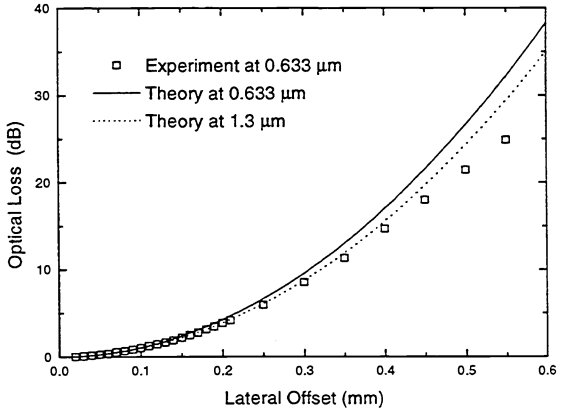

Fig. 5. Optical loss as a function of lateral offset between the two GRIN lenses placed 20 cm apart.

As seen in Fig. 6, the angular tilt misalignment shows the most significant optical loss among the three misalignments. A very small angular tilt such as 0.1° results in 8.4 dB and 1.8 dB optical loss for the wavelengths of 0.6328 μm and 1.3 μm, respectively. For the longer wavelength (1.3 μm), the angular tilt is less sensitive than for the shorter wavelength (0.6328 μm). Again, the separation between the two GRIN rod lenses was 20 cm. The measured optical loss shows the same results as the theoretical calculation for the small angular tilt. As the angle increases, the theory predicts higher loss than measured.

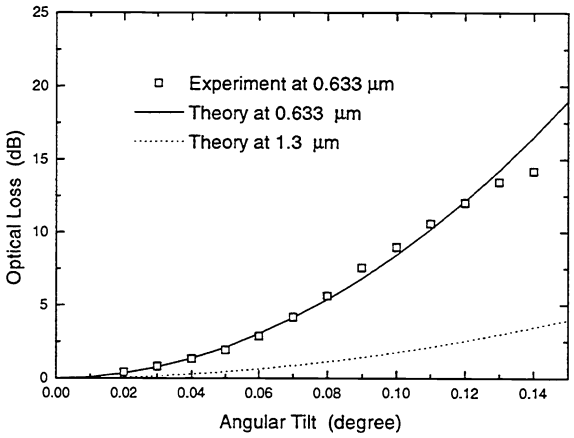

Fig. 6. Optical loss as a function of angular tilt between the two GRIN lenses placed 20 cm apart.

In summary, theoretical and experimental results of alignment losses for the single-mode fiber coupling efficiency with GRIN rod lenses were provided. The next section will provide experimental results using imaging lenses with the GRIN-based fiber coupling approach.

4. FIBER-OPTIC GRIN-BASED COUPLING ISSUES USING EXTERNAL IMAGING LENSES

4.1 Experiments

Fig. 7 shows a schematic diagram of the fiber-optic GRIN-based N-channel interconnect when using two external imaging lenses. The z direction is along the optic axis of the imaging lenses. The x and y directions are parallel to the surface of the source GRIN lenses. The origin of the coordinate space is on the optic axis of the imaging lenses. The spherical imaging lenses are utilized to reduce optical loss for long separation distances between the source and receiving fiber-optic arrays. The focal length of the imaging lens is denoted as F. The separation Z_o denotes the distance between the source and receiving GRIN-rod lenses. In our experiments, a pair of the fiber pigtailed GRIN rod lenses are used and are moved with translation stages to simulate the two physical N channel arrays. Sequence of positions of the GRIN lens source is at x = 0, -1.8, -3.6, -5.4, -7.2, -9, -10.8, -12.6, and -14.4 mm, for taking the optical power measurements. The distance of 1.8 mm between channels corresponds the diameter of GRIN lens. The same GRIN lenses described in the previous section were used. A pair of plano-convex lenses from Melles Griot (BK-7, Diameter: 101.6 mm, F = 25.4 cm) were used for the external imaging lenses. The separation Z_o between the two GRIN lenses is equal to 101.6 cm since a 4F 1:1 imaging system is utilized.

As shown in Fig. 8, normalized optical power at the end of the receiving fiber was measured as a function of the position of the receiving fiber-optic GRIN assembly. The positions of the receiving fiber where peak values were measured (x = 0, 1.8, 3.6, 5.4, 7.2, 9, 10.8, 12.6, and 14.4 mm) matched the positions of the source fiber in the opposite x direction due to the reversed channel order at the receiving assembly. The measured optical power is normalized with the peak power in the channel on the optic axis. The lenses have a 0.8 dB optical loss since they are not antireflection coated. Due to this loss, the measured peak power on the axis was lower by 0.8 dB compared to the measured power with the perfect alignment when no imaging lenses were used. Coupling efficiency for each channel in the receiving array is not uniform due to the spherical aberration present in our imaging lenses. As seen in Table 1, variation of the peak optical power between channels is

calculated as $10\log(\frac{P_j}{P_1})$ where P_j is peak optical power in the jth channel, and P_1 is the peak optical power in the channel on the optic axis. Maximum variation of 0.55 dB is obtained between the first and the ninth channel. The minimum physical inter-channel distance is determined when the GRIN-rod lenses are attached to each other without any air gap. Crosstalk between the two adjacent channels is below measurement range when the source and receiving GRIN lenses with diameters of 1.8 mm are placed at the minimum physical inter-channel distance of 1.8 mm. A minimum measurable optical crosstalk of less than -56dB was obtained when the lateral offset of the receiving GRIN lens is 0.9 mm. This is equivalent to a RF (electrical) crosstalk level of < -112 dB.

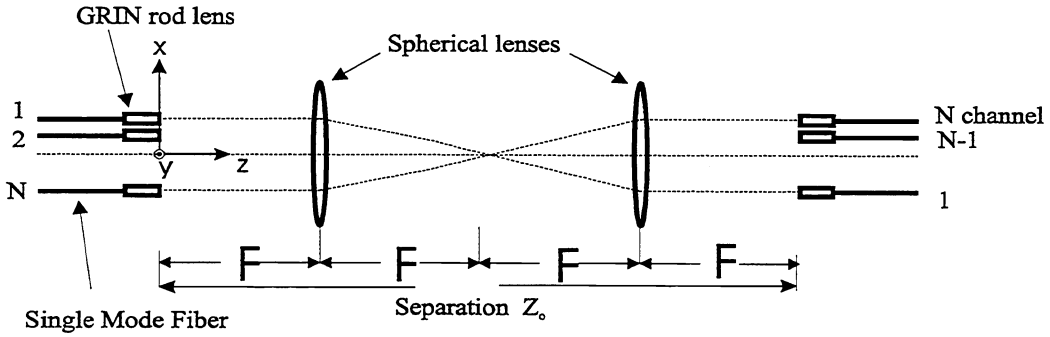

Fig. 7. Schematic diagram of fiber-optic GRIN-based interconnect using external imaging lenses.

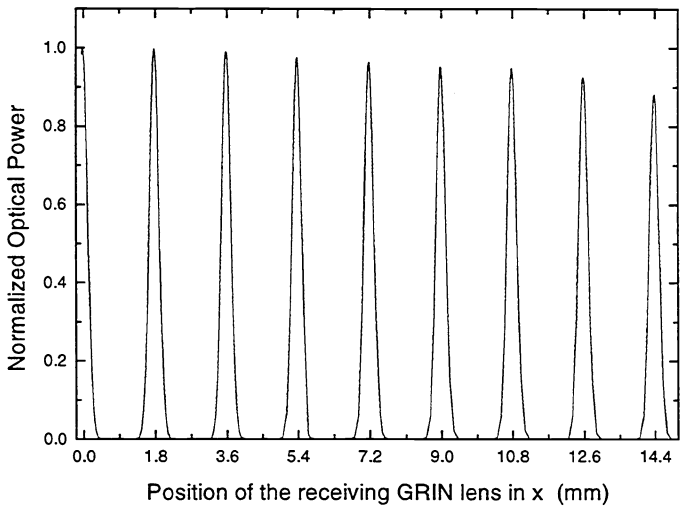

Fig. 8. Measured optical power at the end of the receiving fiber as a function of the position of the receiving fiber-optic GRIN assembly. Here 4F = 101.6 cm.

Table 1. Variation of peak optical power in each channel with respect to the power in the optic axis channel. Here 4F = 101.6 cm.

Channel #	Variation (dB)
1	0
2	-0.011
3	-0.032
4	-0.095
5	-0.16
6	-0.215
7	-0.237
8	-0.338
9	-0.547

Fig. 9 shows measured optical loss as a function of the angular tilt misalignment between the two fiber-GRIN assemblies when using the two external imaging lenses. The source GRIN-rod lens was fixed along the optic axis. The experimental angular tilt misalignment sensitivity of the receiving GRIN rod lens proved to be severe, and an accurate angle alignment, i.e., <0.1 degree, was required to obtain an optical loss of less than 5 dB.

Fig. 10 shows measured optical loss as a function of the separation misalignment between the two fiber-GRIN assemblies when using the two external imaging lenses. As shown experimentally, optical loss due to the separation misalignment error ΔZ_o is small due to the imaging lenses. For a separation misalignment error ΔZ_o= 5 mm or a $\Delta Z_o/Z = 0.5/101.6 \approx 0.5\%$ error, the optical loss is very small, i.e., < 0.1 dB.

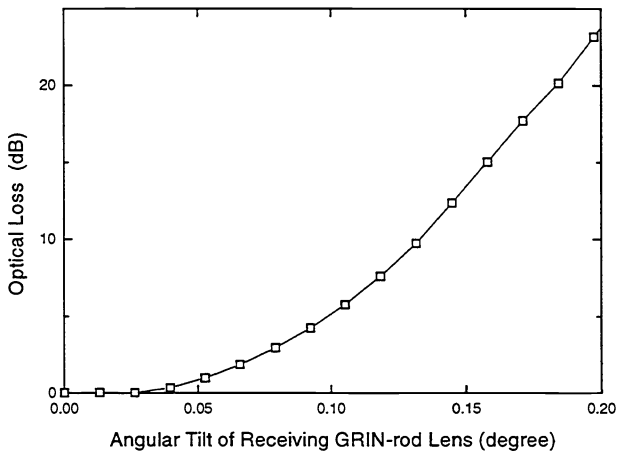

Fig. 9. Measured optical loss as a function of the angular tilt misalignment between the two fiber-GRIN assemblies with the external imaging lenses, with 4F = 101.6 cm.

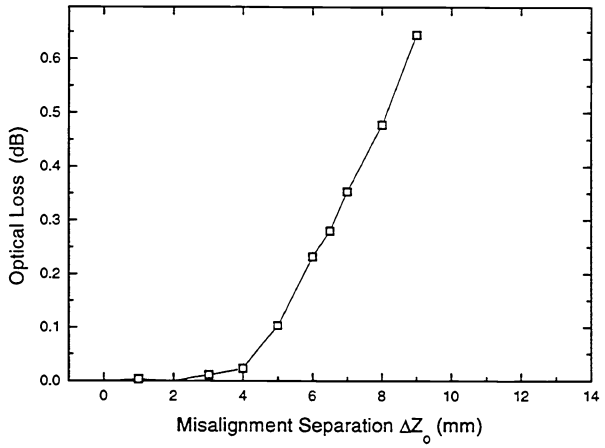

Fig. 10. Measured optical loss as a function of separation misalignment $\Delta Z_{o,}$, with $Z_o = 4F = 101.6$ cm.

5. DESIGN OF THE 2-D FIBER-OPTIC LENS ARRAY

Fig. 11 shows a schematic diagram of a fiber array interconnect using a micro-lens array substrate and a fiber-array-holder substrate. There are various design options to realize this structure. A microlens array, a Fresnel lens array, or a GRIN lens array can be utilized for the micro-lens array to collimate guided light in the air. In this paper, the GRIN lens array approach is studied since the GRIN lenses have a good collimating property, with good aberration correction characteristics, and a convenient geometric shape [4]. The fiber-holder can be fabricated by stacking V-grooved wafers to provide alignment along two lines of contact with the fiber. V-grooves provide a high degree of horizontal confinement. Another possible method for fabrication of the fiber-holder is to utilize X-ray lithography such as the LIGA process [10]. LIGA is a German acronym for Lithographie, Galvanoformung, Abformung which translates to X-ray Lithography, Electroplating and Plastic Molding. Using the LIGA process, an arrayed substrate with deep holes to hold the bare fiber and a lens array may be fabricated. In this paper, we discuss mature V-groove technology for the fiber array.

5.1 Design of the 2-D GRIN-Lens-Based Array

As seen in Fig. 12, a hexagonal array geometry using stacked GRIN lenses can be utilized to increase the packing density of the channels in the photonic control unit. As stated in section 4.1 of this paper, we experimentally demonstrated no measurable optical crosstalk between the two adjacent stacked GRIN-based receiving channels. Also, diffraction of the Gaussian beam out of the GRIN rod lens is small; so many optical components such as polarizers, polarization switching-based spatial light modulators (SLMs), and polarizing beamsplitters, can be placed between the source and receiving GRIN assemblies. The pixel size in the SLM can be designed to be the same as the diameter of the GRIN rod lens. H and W denote height and width of the array area, respectively. GRIN lenses from NSG (lens radius R_o =0.9 mm) can be stacked together since their outer diameters have values of 1.8 $\pm$ 0.005 mm, implying a very small ± 5 μm position error tolerance. The variation in GRIN rod lens in lengths and diameters can be minimized by grouping GRIN lenses from the same fabrication batch and by polishing the surfaces of the stacked GRIN lenses together. Antireflection coating can be deposited on the large surface of the GRIN lens array.

The fiber channel density is defined as the total number N_T of GRIN lenses in the area WH. The total number of fiber channels can be calculated as follows

$$N_T = N_W N_H - (N_H - 1)/2, \quad \text{when } N_H \text{ is odd,}$$
$$\text{and} \quad N_T = N_H N_W - N_H/2, \quad \text{when } N_H \text{ is even,} \tag{9}$$

where N_H and N_w are the maximum numbers which satisfy the equations

$$H > R_o [(N_H-1)\tan(60^o) +2],$$
$$\text{and} \quad W > 2 R_o N_w, \tag{10}$$

respectively. As an example, N_T's per square inch are 216 and 68, respectively, when R_o =0.9 mm (bare GRIN lens) and R_o = 1.5 mm (metal jacketed GRIN lens). When the metal jacketed GRIN lens with the pigtailed fiber is used, the fiber-holder assembly is not required. However, the alignment of each fiber to its GRIN lens within a certain tolerance, particularly for all the fiber-pigtailed GRIN lenses in the array is a difficult task. Therefore, the bare GRIN lens array is a better design option in terms of both fabrication and tolerance. The expressions (eqns. 9-10) for the channel density can be used for any type of microlens array and not just the GRIN-rod lens array. For the exact alignment of the channels, a microlens array using photolithography fabrication techniques is desirable, however, design and fabrication of the microlens array with special care to minimize aberrations should be studied.

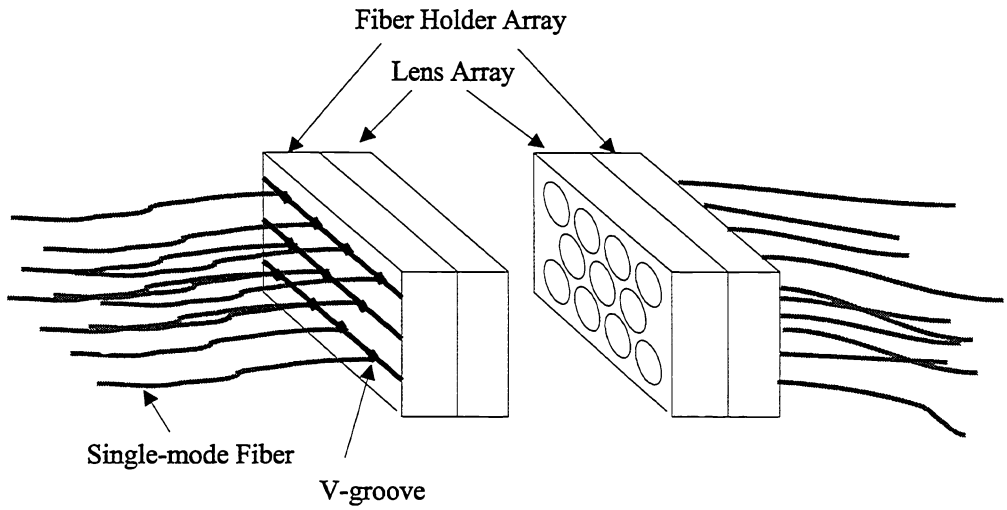

Fig. 11. Schematic diagram of fiber array interconnects using microlens or GRIN rod lens array assemblies.

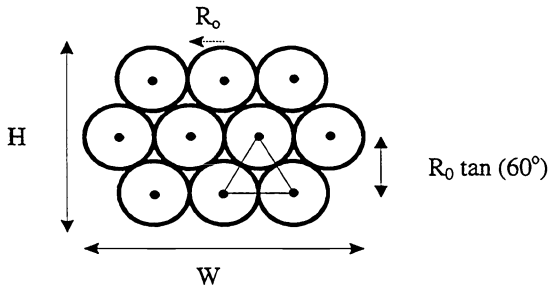

Fig. 12 A hexagonal array geometry using the GRIN-fiber assembly.

5.2 Design of the V-Grooved 2-D Fiber Array

The V-grooves on the silicon wafers can be used for aligning bare optical fibers to the 2-D GRIN-rod lens array [11]. The bare fibers can be sandwiched by two identical sets of V-grooved substrates. The etch rate of a silicon wafer is much greater in the <100> direction than in the <111> direction when a (100) surface silicon covered oxide mask is immersed into a basic solution. A precise V-groove can be obtained due to this anisotropic etching of the silicon [12]. Fig. 13 shows a geometry of a 2D V-grooved fiber array. The width of a V-groove opening, W, can be calculated by applying the equation

$$W=\frac{1}{\tan\theta}(t+\frac{2r_o}{\cos\theta}-\sqrt{3}R_o), \tag{11}$$

where θ (=54.7456°) is the angle of the V-groove, and t, r_o, and R_o are the thickness of the silicon wafer, the radius of the single-mode fiber, and the radius of the GRIN-rod lens (or distance from center-to-center of two adjacent lenses), respectively. The variables g and D as shown in Fig. 13 are the gaps between the two substrates and the vertical distance between the adjacent fiber centers, respectively. When R_o = 900 μm and r_o = 62.5 μm, W is a value between 102.06 μm and 153.09 μm. The corresponding wafer thickness is a value between 1486.67 μm and 1558.85 μm. These precise V-groove structures can be fabricated via crystallographic perfection of the substrate, accurate alignment of the etch pattern with respect to the crystal planes, and optimized etch conditions. For a worst-case situation, a positioning error of the optical fibers of 1.96 μm has been reported [12]. In addition, this V-groove technique can be used to hold GRIN rod lenses, thus resulting in an accurate alignment. To fabricate the V-grooves, the steps below can be followed [13]:

1. Design and make a negative chrome (Cr) mask for the V-groove pattern.
2. Deposit about 300 nm of silicon dioxide (SiO_2)on a (100) silicon wafer where the V-grooves are to be made.
3. Pattern V-groove array pattern with photoresist onto samples using standard lithography techniques.
4. Make a SiO_2 mask by etching the SiO_2 layer with a 6:1 buffer oxide etch (BOE) solution (etch rate of roughly 100 nm/min). The BOE will etch the SiO_2 that is not predicted by the photoresist pattern.
5. Remove the photoresist from the samples after the SiO_2 mask has been formed.
6. Immerse the sample into sodium hydroxide (NaOH), potassium hydroxide (KOH), or cesium hydroxide (CsOH; etch rate at room temperature is about 1 μm/min.) and let it etch until the V-groove is satisfactorily formed.

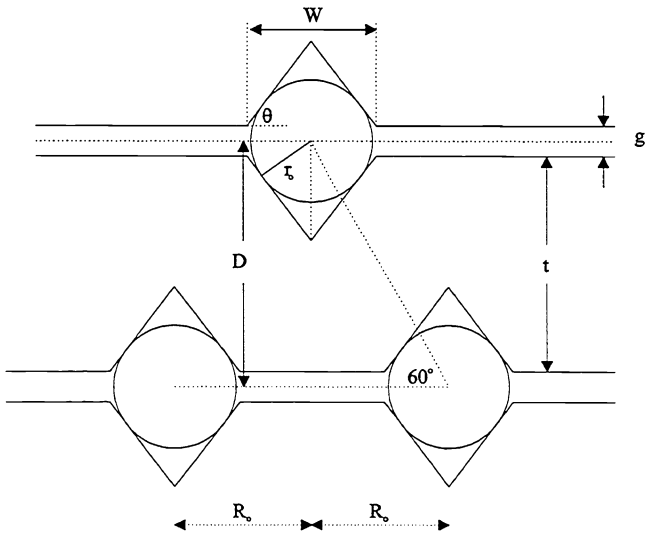

Fig. 13 Geometry of a 2-D V-grooved fiber array.

6. CONCLUSION

We have quantified the critical alignment loss issues for the single-mode fiber coupling geometry with GRIN rod lenses. The critical alignment factors that determine optical loss are lateral offset, separation, and angular tilt between the two fiber-GRIN lens assemblies. The angular tilt misalignment is the most important factor in coupling loss control. For a long separation between two GRIN lenses, the collimated light experiences diffraction, resulting in optical coupling loss. To reduce the separation coupling loss, we have studied optical coupling efficiency issues when using single-mode fiber-GRIN input and output assemblies with external imaging lenses. Optical crosstalk measured between two minimum-physical-distance (i.e., 1.8 mm) adjacent channels in the photonic unit was below the measurement detector sensitivity range (i.e., <-60 dB) when GRIN rod fiber arrays with imaging lenses were used. Coupling efficiency over the channels was not uniform due to spherical aberrations in our experimental imaging lenses. However, the variation was less than 0.6 dB for the ninth channel when compared to the center channel. An accurate angle alignment (i.e., <0.1 degrees) between the two array assemblies is required to obtain an optical loss of less than 5 dB. In contrast, the separation misalignment loss is relatively small. Based on our experimental results, a typical design for a 2-D fiber-optic microlens array has been provided. A hexagonal array geometry of the photonic control unit channels using a GRIN-fiber array can be utilized to increase the channel packing density of the overall photonic unit. Also, a similar pixel size and structure must be designed for the spatial light modulator switching arrays that match the 2-D fiber-optic lens assembly design. In addition, a very precise fiber array holder design has been proposed using a V-groove silicon wafer. Future work includes the evaluation of multi-mode fibers versus single-mode fibers for our remotely controlled photonic beamformer application.

7. ACKNOWLEDGEMENT

The authors would like to acknowledge support from the Office of Naval Research, grant #N000149510988, Program Monitor, Dr. Miceli.

8. REFERENCES

[1] N. A. Riza, "Liquid crystal-based optical time delay units for phased array antennas," *IEEE/OSA Journal of Lightwave Technology*, Vol. 12, No. 8, pp. 1440-1447, August 1994.
[2] N. A. Riza, "Liquid crystal-based optical controllers for phased array antennas," *SPIE* Vol. 2155, pp. 169-179, Los Angeles, 1994.
[3] N. A. Riza and N. Madamopoulos, "Photonic time delay beamforming architecures using polarization switching arrays," *SPIE Conference Proceedings* , Vol. 2754, Orlando, April 1996.
[4] SELFOC Product Guide, Nippon Sheet Glass Co., Ltd., Tokyo, Japan.
[5] D. Marcuse, "Loss analysis of single-mode fiber splices," *Bell Syst. Tech. J.* Vol. 56, pp. 703-718, 1977.
[6] R. W. Gilsdorf and J. C. Palais, "Single-mode fiber coupling efficiency with graded-index rod lenses," *Applied Optics,* Vol. 33, No. 16, pp. 3440-3445, 1994.
[7] F. L. Thiel and R. M. Hawk, "Optical waveguide cable connection," *Applied Optics,* Vol. 15, No. 11, pp. 2785-2791, 1976.
[8] A. Yariv, *Optical Electronics*, 3rd ed. (Holt, Rinehart & Winston New York, 1985), Chap. 2, pp. 23-24.
[9] N. A. Riza, "25-channel nematic liquid-crystal optical time delay unit characterization," *IEEE Photonics Technol. Lett.* Vol. 7, No. 11, pp. 1285-1287, 1995.
[10] K. H. Brenner, M. Kufner, S. Kufner, J. Moisel, A. Muller, S. Sinzinger, M. Testorf, J. Gottert, J. Mohr, "Application of three-dimensional micro-optical components formed by lithography, electroforming, and plastic molding," *Applied. Optics,* Vol.32, No.32, pp.6464-9, 1993.
[11] C. M. Miller, " Fiber-optic array splicing with etched silicon chips," *Bell System Tech J.* Vol. 57, pp. 75-90, 1978.
[12] C. M. Schroeder, "Accurate silicon spacer chips for an optical fiber cable connector," *Bell System Tech J.* Vol. 57, pp. 91-97, 1978.
[13] M. L. Jones, private communication, Georgia Institute of Technology, Atlanta Georgia, 1995.